PHYSICAL REVIEW A **87**, 031401(R) (2013)

Quantum interference and multielectron effects in high-harmonic spectra of polar molecules

A. Rupenyan, P. M. Kraus, J. Schneider, and H. J. Wörner*
Laboratorium für Physikalische Chemie, ETH Zürich, Wolfgang-Pauli-Strasse 10, 8093 Zürich, Switzerland
(Received 16 August 2012; published 8 March 2013)

We experimentally and theoretically analyze the manifestations of quantum interference and multiple ionization channels (multiple orbitals) in high-harmonic spectra of aligned N_2O molecules. Increasing the probe wavelength from 1.17 to 1.46 μm, we demonstrate the gradual disappearance of multielectron effects and quantitatively explain the observation through calculations. We thus identify a minimum in the high-harmonic spectrum of N_2O caused only by its structure. By comparing its position with that measured in the isoelectronic CO_2 molecule for similar axis distributions, we find a difference of 10 eV, confirmed by *ab initio* quantum scattering calculations. Quantum interference in photorecombination is thus shown to be sensitive to subtle differences in the valence orbital structure of molecules with nearly identical lengths. This property may find applications in time-resolved studies.

DOI: 10.1103/PhysRevA.87.031401 PACS number(s): 33.20.Xx, 42.50.Hz, 42.65.Ky

High-harmonic spectroscopy (HHS) provides a new approach to investigating electronic structure and dynamics on femtosecond to attosecond time scales. In spite of important breakthroughs, seemingly simple molecules such as CO_2 and N_2 are still the object of debates [1–11]. A minimum observed in spectra of aligned CO_2 has first been interpreted in terms of *quantum interference* between the recombining photoelectron and the two-center structure of the highest-occupied molecular orbital (HOMO) [2,3,10,11]. However, a molecule exposed to a strong laser field can be ionized to several electronic states of the cation [6,12–15], opening multiple channels for high-harmonic emission. Accordingly, the minimum in CO_2 has later been attributed to *electromagnetic interference* between high-harmonic emission from multiple ionization channels of the molecule [6,8,16]. Using laser pulses with longer wavelengths (1.45–1.7 μm), new evidence for a structural origin of the minimum has been obtained [9], in apparent contrast with previous results obtained in the wavelength range of 0.8–1.3 μm [6,8,16]. Progress in high-harmonic spectroscopy will rely on achieving a better understanding of the sensitivities and mechanisms of the method.

In this Rapid Communication, we study the roles of quantum interference and multiple ionization channels in HHS of aligned weakly polar N_2O molecules that we compare with the apolar isoelectronic CO_2 molecules. We hereby address two questions: (1) What are the conditions under which quantum interference is observed? and (2) What is the relative role of the nuclear geometry and the electronic structure in defining the position of the associated spectral minima?

We answer the first question by studying high-harmonic spectra of N_2O molecules over a range of intensities and wavelengths (1.17–1.46 μm). We show that the position of the previously observed minimum in N_2O [17] is intensity dependent at 1.17 μm, owing to the interference of emission from multiple ionization channels, and that these multielectron effects progressively disappear with increasing wavelength. We quantitatively explain this observation through calculations [6,18], which we extend to polar molecules. Recently, the phenomenon of quantum interference in polar molecules has been studied theoretically [19–21], but the role of multiple ionization channels has not been considered yet.

We answer the second question by comparing the purely structural signatures of two isoelectronic molecules with nearly identical length (2.31 Å in N_2O vs 2.32 Å in CO_2 [22]) but different orbital shapes. In the scattering-wave description of photorecombination [18,23] both the structure of the orbital and that of the scattering potential play a role in determining the positions of quantum interference minima, implying a sensitivity to both the electronic and the nuclear structures. In the present study, we find that the different minimum positions in N_2O and CO_2 reveal subtle differences of their HOMOs although the molecules have nearly identical lengths. We thus conclude that the electronic structure of N_2O and CO_2 dominates in determining the position of the structural minima. The results obtained by comparing two isoelectronic molecules over a wide range of experimental conditions thus allow us to disentangle the roles of the geometric structure, the electronic structure, and multielectron effects which might be useful for time-resolved applications [15,24–26].

The experimental setup consists of a Ti:sapphire laser system, an optical parametric amplifier (Light Conversion, TOPAS-HE), and a vacuum chamber. The laser system (8 mJ, 28 fs, 1 kHz) provides pulses centered at 0.8 μm which traverse an 80:20 beam splitter. The more intense beam is used to pump the TOPAS-HE that generates tunable infrared (IR) pulses in the range 1.1–1.5 μm with measured pulse durations of 40–50 fs. The minor part of the output is stretched to 120 fs and used for nonadiabatic alignment of the molecules. The mid-IR probe beam is aligned parallel to the 0.8-μm pump beam with a vertical offset of 0.7 cm and the two beams are focused into a gas jet inside a vacuum chamber using an $f = 50$-cm spherical mirror. The molecular beam is generated by supersonic expansion through a pulsed valve with a 250-μm orifice and a backing pressure of 5 bars. The focused laser beams intersect the gas jet 2–3 mm downstream from the nozzle. The high harmonics generated by the probe beam propagate into a spectrometer consisting of a 120-μm-wide entrance slit, a concave aberration-corrected grating (Shimadzu, 30-002), and an extended-dynamic-range

*woerner@phys.chem.ethz.ch; www.atto.ethz.ch

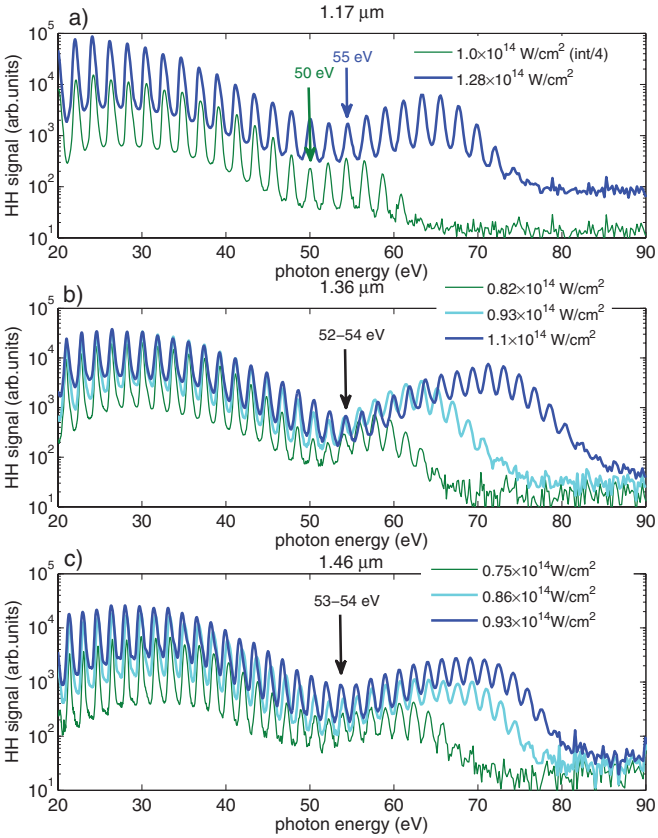

FIG. 1. (Color online) High-harmonic spectra generated in transiently aligned N_2O molecules with 40–50 fs laser pulses of central wavelengths 1.17 μm (a), 1.36 μm (b), and 1.46 μm (c) and a range of intensities indicated in the legends. The spectra recorded at the lowest intensity in each panel are indicated by a thin dark green (gray) line, and the highest by a thick dark blue (gray) line. The arrows indicate the positions of the observed minima.

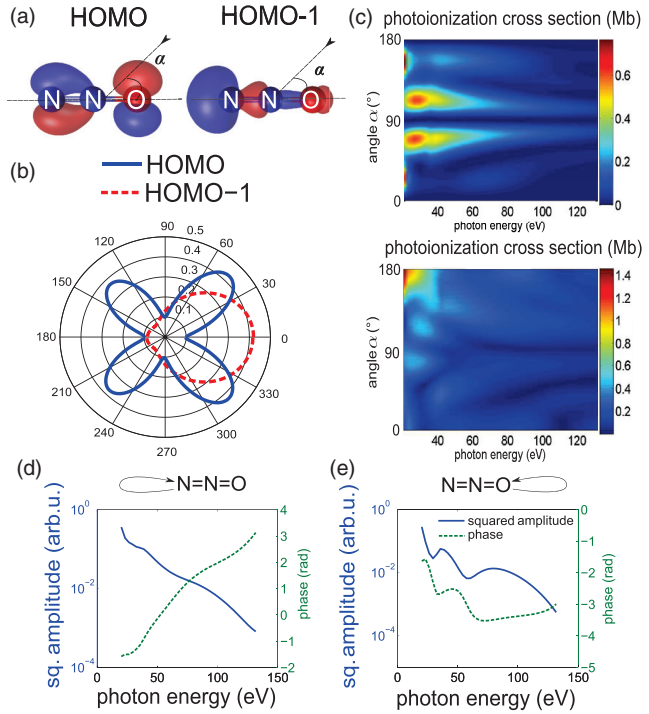

FIG. 2. (Color online) (a) HOMO and HOMO-1 orbitals of N_2O from a HF calculation using a cc-pVTZ basis set. (b) Angular variation of the strong-field ionization rates of the HOMO (solid line) and HOMO-1 (dashed line) orbitals calculated for an intensity of 1.0×10^{14} W/cm^2. (c) Photoionization cross sections of HOMO (top panel) and HOMO-1 (bottom panel) as a function of the emitted photon energy and the electron emission angle α in the molecular frame. (d), (e) Calculated squared amplitude (solid line) and phase (dashed line) of the induced dipole moment for recombination from a single side of the molecule, using a typical axis distribution characterized by $\langle \cos^2 \theta \rangle = 0.60$.

microchannel-plate detector backed with a phosphor screen (Photonis, 37258). In the present study, we have not observed orientation under the same experimental conditions used to orient OCS [27], which we attribute to the weak polarity of N_2O.

Figure 1 shows high-harmonic spectra of N_2O molecules aligned parallel to the polarization direction of the probe beam for the three wavelengths 1.17 μm (a), 1.36 μm (b), and 1.46 μm (c) and several intensities given in the legends. The molecules were impulsively aligned using a 120-fs, 0.8-μm pulse and were recorded at the first half-revival of the rotational dynamics. All spectra show distinct minima in the range of 50–55 eV. At the shortest wavelength, the minimum position changes with the intensity of the probe pulse, moving from 50 to 55 eV. At 1.36 and 1.46 μm the position of the minimum moves by less than 2 eV. We thus observe a progressive decrease of the intensity dependence of the minimum in N_2O with increasing wavelength of the probe pulse for similar relative variations of the probe intensity. This situation is reminiscent of CO_2 where such a result was, however, obtained in different studies using very different laser sources [8,9,16]. Here, we show that the intensity dependence of the minimum position disappears toward longer wavelengths even when relatively long pulses (consisting of 7-9 cycles) are used. We show that the same is true for CO_2 molecules in a companion paper [28].

We now discuss our theoretical model (details are given in Ref. [28]). The valence electronic structure of N_2O consists of the orbitals with the following symmetries and binding energies (equal to the vertical ionization energies within Koopmans' theorem): π, 12.89 eV; σ, 16.38 eV; π, $\sim$18.2 eV; and σ, 20.11 eV [29]. Both ionization from and recombination to HOMO are suppressed when the molecule is aligned parallel to the generating laser field. Therefore, the contribution of HOMO-1 becomes significant and is fully included in our model. Lower-lying orbitals (HOMO-2 and HOMO-3) were found to contribute insignificantly and were not included in the calculations.

We use a velocity-gauge model for strong-field ionization [6,30,31] and extend it to take into account the polarity of N_2O and the Stark effect. Our model thus incorporates the directional dependence of the effective binding energy resulting from the Stark effect, as, e.g., in Ref. [32]. The polarization of the orbitals, which becomes important in systems with large polarizabilities [33], is not included here. The orbitals were obtained from a Hartree-Fock calculation using a correlation-consistent polarized valence-triple-ζ (cc-pVTZ) basis set and are shown in Fig. 2(a). The permanent

dipole moments and polarizabilities were obtained by fitting a second-order polynomial to the orbital binding energies obtained from an MP2 calculation with an applied static field in the range of 0–0.1 atomic units. The resulting tunnel-ionization rates for the HOMO and HOMO-1 of N_2O are shown in Fig. 2(b). Whereas the ionization rate of HOMO is essentially inversion symmetric, the ionization rate of HOMO-1 is strongly asymmetric, with a maximum amplitude for removing the electron via the oxygen atom. This asymmetry is dominated by the permanent dipole moment of the orbital, in analogy to OCS [34].

We use the strong-field approximation [35] to calculate channel-specific continuum electron wave packets. These wave packets contain all laser-pulse-specific properties of high-harmonic emission. In particular, the relative phase contributed by the propagation step as a consequence of different ionization potentials (I_p), which is sometimes approximated by $\Delta I_p \tau$ with τ the transit time of the electron [8,36,37], is naturally included in the spectral phase of the continuum electron wave packets. We model photorecombination using *ab initio* quantum scattering calculations [38,39] based on the Hartree-Fock orbitals described above. The calculated photoionization cross sections are shown in Fig. 2(c). Finally, we calculate the total induced dipole moment at photon energy Ω of an ensemble of molecules partially aligned along the direction of the probe field as follows:

$$d(\Omega) = \int_0^\pi d\theta \, \sin\theta A(\theta) \sum_i \sqrt{I_i(\theta)} a_{ewp,i}(\Omega) d_{\mathrm{rec},i}(\Omega,\theta), \tag{1}$$

where θ is the angle between the molecule and the polarization direction of the probe field, i runs over the relevant ionization channels (ionization from HOMO or HOMO-1), $A(\theta)$ is the axis distribution, I_i is the strong-field ionization rate, $a_{ewp,i}$ is the complex photoelectron wave packet, and $d_{\mathrm{rec},i}$ are the complex recombination matrix elements described above.

We illustrate these theoretical results by first restricting the calculations to the HOMO channel and using $a_{ewp}(\Omega) = 1$ with a typical axis distribution ($\langle\cos^2\theta\rangle = 0.60$, taken from Ref. [40]). Figure 2(d) shows the obtained squared amplitude and phase with photorecombination restricted to the N side ($\alpha = +90^\circ$ to $+270^\circ$) and Fig. 2(e) for recombination from the O side ($\alpha = -90^\circ$ to $+90^\circ$). Photorecombination from the O side leads to two distinct minima and associated phase variations at 29 and 59 eV, respectively, whereas recombination from the N side is characterized by a structureless spectral amplitude and phase. These results differ markedly from the plane-wave approximation of the continuum that yields photorecombination matrix elements from the two sides that are simply complex conjugates of each other [19–21,41]. The substantial differences between recollision from the two sides are thus the result of the asymmetric diffraction of the photoelectron wave packet in the molecular potential prior to recombination. Minima are thus only found to occur in the emitted spectra when the electron wave packet first encounters the oxygen atom rather than the nitrogen atom, revealing an interesting sensitivity of photorecombination to molecular asymmetries.

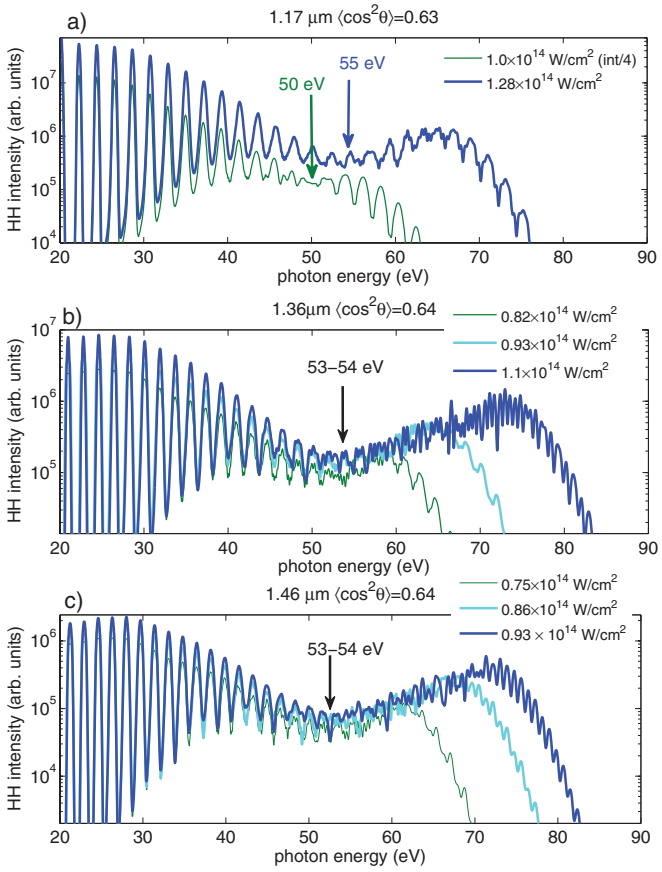

FIG. 3. (Color online) Calculated high-harmonic spectra including the HOMO and HOMO-1 channels using the quantities shown in Fig. 2 and calculated photoelectron wave packets. Wavelengths, intensities, and pulse durations are chosen according to the experimental conditions of Fig. 1. The spectra recorded at the lowest intensity in each panel are indicated by a thin dark green (gray) line, and the highest by a thick dark blue (gray) line. The degree of axis alignment ($\langle\cos^2\theta\rangle$) has been slightly adjusted to reproduce the experimental spectra and is indicated in each panel.

The results of calculations using Eq. (1) with both channels and the experimental conditions used in Fig. 1 are shown in Fig. 3. For all wavelengths and intensities the minimum positions and their intensity dependence are well reproduced. The analysis of the calculations, which is presented in detail elsewhere [28], shows that the minimum position is found to depend most strongly on the intensity when probe pulses with short wavelengths are used. Under such conditions, the emission from HOMO and HOMO-1 is comparable over a range of harmonics in the cutoff region, which leads to the large shift observed at 1.17 μm. With increasing wavelength and similar intensities, the cut off increases and becomes sharper in the energy domain such that the minima appear in the plateau region of the spectrum, where the contributions from lower orbitals are smaller. This leads to the observed decrease of the intensity dependence observed at 1.36 and 1.46 μm. We have thus shown that our measurements isolate a structural signature of the N_2O molecule in the spectra measured at 1.46 μm and intensities above 0.85×10^{14} W/cm^2.

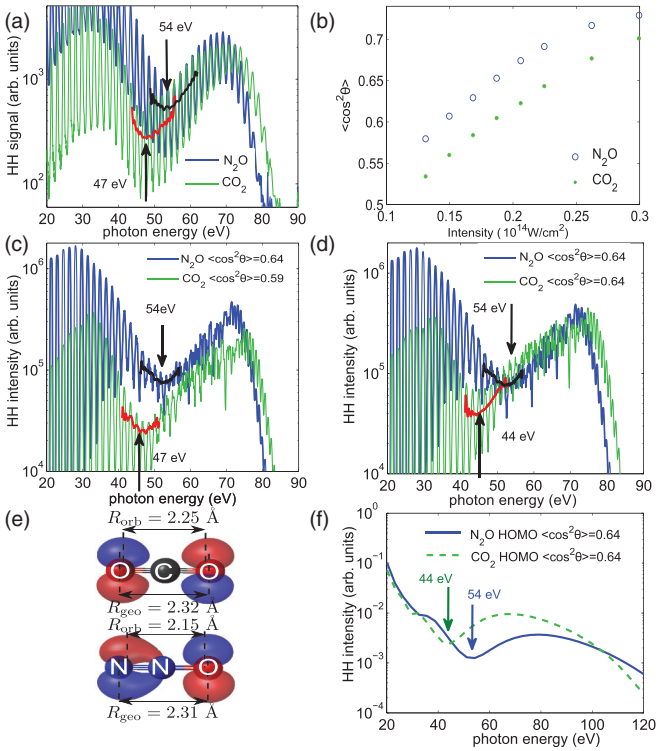

FIG. 4. (Color online) (a) Experimental high-harmonic spectra recorded under identical conditions with a driving wavelength of 1.46 μm. The positions of the minima are highlighted using a smoothed replica of the spectra. (b) Calculated maximal degrees of axis alignment for N_2O [thick blue (gray) line] and CO_2 [thin green (gray) line] for $T_{rot} = 40$ K impulsively aligned by a 120-fs pulse. (c) Calculated spectra with adjusted degrees of axis alignment given in the legend. (d) Calculated spectra using the same axis distribution for both molecules. (e) HOMOs of N_2O and CO_2. (f) Spectral envelope of the high-harmonic emission from the HOMO channel only of N_2O (solid line) and CO_2 (dashed line), assuming an energy-independent photoelectron wave-packet amplitude [$a_{ewp}(\Omega) = 1$].

We now study the origin of this minimum by comparing its position to that observed in CO_2. High-harmonic spectra recorded in aligned CO_2 and N_2O molecules under identical experimental conditions and a wavelength of 1.46 μm are shown in Fig. 4(a). The N_2O spectrum in Fig. 4(a) is the same as that shown in Fig. 1(c) using the highest probe intensity (0.93×10^{14} W/cm^2 determined by comparison with calculations). Before comparing the minimum positions directly, we must take into account the different polarizabilities [42] and therefore slightly different axis distributions of the molecules under identical experimental conditions. Calculations of the rotational dynamics of the two molecules using the experimental parameters (120 fs pulse duration, $T_{rot} = 40$ K, intensity in the range of 2×10^{13} W/cm^2) show that N_2O reaches a consistently higher degree of $\langle\cos^2\theta\rangle$ by 0.04–0.05 compared to CO_2 [Fig. 4(b)]. We thus determine the experimental degrees of alignment in N_2O and CO_2 separately by comparing the observed minimum positions to calculations [Fig. 4(c)]. We obtain a degree of axis alignment of $\langle\cos^2\theta\rangle = 0.59$ and 0.64 for CO_2 and N_2O, respectively, in excellent agreement with the difference expected from the rotational wave-packet calculations. With this knowledge, we can now predict the spectra of CO_2 and N_2O for identical axis distributions [see Fig. 4(d)]. We find that the minimum positions differ by 10 eV.

We now analyze this remarkable finding. The overall length of the molecules is nearly identical with $R_{geo} = 2.312 \pm 0.003$ Å in N_2O and 2.324 ± 0.003 Å in CO_2 [see Fig. 4(e)]. Thus, the traditional two-center model which has been applied to CO_2 and N_2O (e.g., in Refs. [11,17]), cannot explain this difference. However, our model described above quantitatively accounts for this experimental observation in terms of photorecombination to the HOMO. We now look for a physical interpretation of the different minimum positions between CO_2 and N_2O using the two-center interference formula ($n\lambda_{dB} = R\cos\theta$) backwards. With $\theta = 30°$ [which is the alignment angle with the largest contribution in the sense that $A(\theta)\sin(\theta)\sqrt{I(\theta)}$ is maximal] and converting the photon energy (Ω) of the minimum to an electron de Broglie wavelength (λ_{dB}) using $\Omega = 2\pi^2/\lambda_{dB}^2$ (in atomic units), we obtain an internuclear separation of $R = 2.16 \pm 0.10$ Å for CO_2, which is in moderate agreement with the separation R_{geo} of the two O atoms of 2.32 Å [22] [see Fig. 4(e)]. Applying the same approach to N_2O results in $R = 1.94 \pm 0.10$ Å. This deviates even more strongly from the overall length of N_2O of 2.31 Å. However, the separation of the centers of gravity of the orbital lobes of the HOMOs, R_{orb}, amounts to 2.25 ± 0.02 Å for CO_2, and 2.15 ± 0.02 Å for N_2O. Given the simplicity of the model, these numbers are in reasonable agreement with the effective lengths extracted from the experiment. We can therefore attribute the difference in the observed minimum positions to the shorter separation of the orbital lobes in the HOMO of N_2O and to the deviation of the orbital from a simple two-center model. This result is demonstrated more rigorously in Fig. 4(f) where the difference in the minima is adequately predicted by the pure HOMO emission channel for both molecules.

In conclusion, we have thus shown signatures of ionization from lower orbitals in high-harmonic spectra of N_2O and the disappearance of this effect with increasing wavelength under otherwise identical conditions. This observation has been rationalized through the position of the observed minimum relative to the high-harmonic cutoff and the associated relative emission strength from different channels, as demonstrated in a full theoretical model. This approach enabled us to experimentally isolate the structural minimum in N_2O and to compare it with that in CO_2. Taking the different axis distributions into account, we then showed that the minimum is located $\sim$10 eV higher in N_2O than in CO_2, although the molecules have nearly identical lengths, which is validated by our *ab initio* calculations. Using the weakly polar N_2O molecule, we have thus shown that quantum interference in polar molecules distinguishes electronic structure from nuclear geometry. This insight may have important implications in applying high-harmonic spectroscopy to ultrafast photochemical dynamics [26,43], suggesting that the technique might discern between electronic and nuclear rearrangements. This would be particularly useful in the case of vibronic coupling, which is ubiquitous in the dynamics of polyatomic molecules.

We gratefully acknowledge funding from the Swiss National Science Foundation (PP00P2_128274), ETH Zürich (ETH-33 10-3 and Postdoctoral Fellowship Program), and the Marie Curie COFUND program.

[1] J. Itatani, J. Levesque, D. Zeidler, H. Niikura, H. Pépin, J. C. Kieffer, P. B. Corkum, and D. M. Villeneuve, Nature (London) **432**, 867 (2004).

[2] T. Kanai, S. Minemoto, and H. Sakai, Nature (London) **435**, 470 (2005).

[3] C. Vozzi, F. Calegari, E. Benedetti, J.-P. Caumes, G. Sansone, S. Stagira, M. Nisoli, R. Torres, E. Heesel, N. Kajumba *et al.*, Phys. Rev. Lett. **95**, 153902 (2005).

[4] W. Boutu, S. Haessler, H. Merdji, P. Breger, G. Waters, M. Stankiewicz, L. J. Frasinski, R. Taieb, J. Caillat, A. Maquet *et al.*, Nat. Phys. **4**, 545 (2008).

[5] X. Zhou, R. Lock, W. Li, N. Wagner, M. M. Murnane, and H. C. Kapteyn, Phys. Rev. Lett. **100**, 073902 (2008).

[6] O. Smirnova, Y. Mairesse, S. Patchkovskii, N. Dudovich, D. M. Villeneuve, P. B. Corkum, and M. Y. Ivanov, Nature (London) **460**, 972 (2009).

[7] S. Haessler, J. Caillat, W. Boutu, C. Giovanetti-Teixeira, T. Ruchon, T. Auguste, Z. Diveki, P. Breger, A. Maquet, B. Carre *et al.*, Nat. Phys. **6**, 200 (2010).

[8] H. J. Wörner, J. B. Bertrand, P. Hockett, P. B. Corkum, and D. M. Villeneuve, Phys. Rev. Lett. **104**, 233904 (2010).

[9] C. Vozzi, M. Negro, F. Calegari, G. Sansone, M. Nisoli, S. De Silvestri, and S. Stagira, Nat. Phys. **7**, 822 (2011).

[10] K. Kato, S. Minemoto, and H. Sakai, Phys. Rev. A **84**, 021403 (2011).

[11] R. M. Lock, S. Ramakrishna, X. Zhou, H. C. Kapteyn, M. M. Murnane, and T. Seideman, Phys. Rev. Lett. **108**, 133901 (2012).

[12] G. N. Gibson, R. R. Freeman, and T. J. McIlrath, Phys. Rev. Lett. **67**, 1230 (1991).

[13] B. K. McFarland, J. P. Farrell, P. H. Bucksbaum, and M. Gühr, Science **322**, 1232 (2008).

[14] H. Akagi, T. Otobe, A. Staudte, A. Shiner, F. Turner, R. Dörner, D. M. Villeneuve, and P. B. Corkum, Science **325**, 1364 (2009).

[15] J. P. Farrell, S. Petretti, J. Förster, B. K. McFarland, L. S. Spector, Y. V. Vanne, P. Decleva, P. H. Bucksbaum, A. Saenz, and M. Gühr, Phys. Rev. Lett. **107**, 083001 (2011).

[16] R. Torres, T. Siegel, L. Brugnera, I. Procino, J. G. Underwood, C. Altucci, R. Velotta, E. Springate, C. Froud, I. C. E. Turcu *et al.*, Phys. Rev. A **81**, 051802 (2010).

[17] R. Torres, T. Siegel, L. Brugnera, I. Procino, J. G. Underwood, C. Altucci, R. Velotta, E. Springate, C. Froud, I. C. E. Turcu *et al.*, Opt. Express **18**, 3174 (2010).

[18] A.-T. Le, R. R. Lucchese, S. Tonzani, T. Morishita, and C. D. Lin, Phys. Rev. A **80**, 013401 (2009).

[19] X. Zhu, Q. Zhang, W. Hong, P. Lan, and P. Lu, Opt. Express **19**, 436 (2011).

[20] B. B. Augstein and C. F. de Morisson Faria, J. Phys. B **44**, 055601 (2011).

[21] A. Etches, M. B. Gaarde, and L. B. Madsen, Phys. Rev. A **84**, 023418 (2011).

[22] G. Herzberg, *Molecular Spectra and Molecular Structure, Volume III: Electronic Spectra and Electronic Structure of Polyatomic Molecules*, 2nd ed. (Krieger Publishing Company, Malabar, 1991).

[23] H. J. Wörner, H. Niikura, J. B. Bertrand, P. B. Corkum, and D. M. Villeneuve, Phys. Rev. Lett. **102**, 103901 (2009).

[24] M. Lein, Phys. Rev. Lett. **94**, 053004 (2005).

[25] S. Baker, J. S. Robinson, C. A. Haworth, H. Teng, R. A. Smith, C. C. Chirila, M. Lein, J. W. G. Tisch, and J. P. Marangos, Science **312**, 424 (2006).

[26] H. J. Wörner, J. B. Bertrand, B. Fabre, J. Higuet, H. Ruf, A. Dubrouil, S. Patchkovskii, M. Spanner, Y. Mairesse, V. Blanchet *et al.*, Science **334**, 208 (2011).

[27] P. M. Kraus, A. Rupenyan, and H. J. Wörner, Phys. Rev. Lett. **109**, 233903 (2012).

[28] A. Rupenyan, P. M. Kraus, J. Schneider, and H. J. Wörner, Phys. Rev. A **87**, 033409 (2013).

[29] K. Kimura, S. Katsumata, Y. Achiba, T. Yamazaki, and S. Iwata, *Handbook of HeI Photoelectron Spectra* (Japan Scientific Societies Press, Tokyo, 1981).

[30] J. Muth-Böhm, A. Becker, and F. H. M. Faisal, Phys. Rev. Lett. **85**, 2280 (2000).

[31] A. Jaron-Becker, A. Becker, and F. H. M. Faisal, J. Phys. B **36**, L375 (2003).

[32] H. Li, D. Ray, S. De, I. Znakovskaya, W. Cao, G. Laurent, Z. Wang, M. F. Kling, A. T. Le, and C. L. Cocke, Phys. Rev. A **84**, 043429 (2011).

[33] D. Dimitrovski, C. P. J. Martiny, and L. B. Madsen, Phys. Rev. A **82**, 053404 (2010).

[34] L. Holmegaard, J. L. Hansen, L. Kalhoj, S. Louise Kragh, H. Stapelfeldt, F. Filsinger, J. Küpper, G. Meijer, D. Dimitrovski, M. Abu-samha *et al.*, Nat. Phys. **6**, 428 (2010).

[35] V. S. Yakovlev, M. Ivanov, and F. Krausz, Opt. Express **15**, 15351 (2007).

[36] T. Kanai, E. J. Takahashi, Y. Nabekawa, and K. Midorikawa, Phys. Rev. Lett. **98**, 153904 (2007).

[37] H. J. Wörner, J. B. Bertrand, P. B. Corkum, and D. M. Villeneuve, Phys. Rev. Lett. **105**, 103002 (2010).

[38] A. P. P. Natalense and R. R. Lucchese, J. Chem. Phys. **111**, 5344 (1999).

[39] F. A. Gianturco, R. R. Lucchese, and N. Sanna, J. Chem. Phys. **100**, 6464 (1994).

[40] A. Rupenyan, J. B. Bertrand, D. M. Villeneuve, and H. J. Wörner, Phys. Rev. Lett. **108**, 033903 (2012).

[41] A. Etches and L. B. Madsen, J. Phys. B **43**, 155602 (2010).

[42] D. Jonsson, P. Norman, H. Agren, A. Rizzo, S. Coriani, and K. Ruud, J. Chem. Phys. **114**, 8372 (2001).

[43] H. J. Wörner, J. B. Bertrand, D. V. Kartashov, P. B. Corkum, and D. M. Villeneuve, Nature (London) **466**, 604 (2010).